EUROPEAN ORGANISATION FOR NUCLEAR RESEARCH
CERN – A&B DEPARTMENT

AB-Note-2007-037 ABP

Transfer Line Studies from LINAC4 to the PS Booster: Green Field Option

G. Bellodi, A. M. Lombardi

Abstract

Linac4 is a normal conducting H^- linac, which is currently under study at CERN as upgrade to the present LHC injectors chain in view of intensifying the proton flux available for the CERN accelerator complex and eventually attain LHC ultimate luminosity goals. The new linac is designed to accelerate a 65 mA H^- ion beam from 45 keV up to 160 MeV for charge-exchange injection into the CERN Proton Synchrotron Booster, thus overcoming the space charge limitations of the present injection mechanism at 50 MeV, which represent the main obstacle to obtaining higher beam brightness into the PS.
A transfer line is being planned to transport the beam from the end of Linac4 to the PSB: a solution corresponding to a siting of the linac in the existing PS South Hall was initially studied [1] but later discarded in favour of a new "green field" arrangement of a whole complex of new machines (including the SPL and PS2) at CERN. The present note outlines this latest layout and presents the results of the relative beam dynamics studies.

Geneva, Switzerland
September 2007

Introduction

Linac4 [2] is an H^- linear accelerator presently studied at CERN. This machine consists of normal-conducting structures operating at 352.2 MHz and re-using the RF equipment from the decommissioned LEP collider. It is designed to replace the existing Linac2 and to inject the beam into the CERN PS Booster (PSB) at 160 MeV instead of the present 50 MeV injection energy to overcome space-charge limitations. Linac4 is also designed to be a front-end for the future high power 3.5 GeV superconducting linac (SPL) [3].

A new transfer line will have to be built to transport the beam from the end of Linac4 to the PS Booster : this was initially planned to be located in the PS South Hall (building 150), as close as possible to the PSB to minimize the length of the beam transport. However this choice of location was later discarded owing to a string of difficulties attached (to do with engineering, safety, interference with existing machines, commissioning problems etc.). In an effort to come up with a more farsighted and global plan of future development of the LHC injectors, a green-field solution has been recently laid out for the location of a proposed new chain of machines feeding the LHC, which comprises Linac4, the SPL and PS2 [4] (see Fig.1). The new siting is hence not only open to further upgrade possibilities beyond Linac4 energies (which was not the case for the South Hall option), but can also guarantee a virtual uninterruption of physics at the time of commissioning due to the possibility of switching between machines. As a result of some optimisation of the SPL location, the transfer line transporting the beam from the end of Linac4 to the PS Booster is envisaged to be built in an area in the vicinity of the Mont Citron, beneath which the Linac4 tunnel will be located. Some layout constraints have descended from this choice and from the chosen orientation of the Linac4-SPL line, in particular the necessity to adopt a "winding" layout with an initial angle between the linac and the transfer line and a second bend downstream where the transfer line connects with the existing line going from Linac2 to the PSB. The scheme described in this note refers to a 'flat' version of the transfer line, on the same level as Linac2 and the PSB; an updated design, motivated by a recent decision to lower the Linac4 machine tunnel by 2.5m, is going to be published soon.

Layout

In the present scheme the Linac4 transfer line layout can be conceptually divided in two parts: in the second one, it just follows the outline of the existing Linac2 transfer line from the position of the LT.BHZ20 bending magnet up to the Booster injection point (see Fig.16). In its initial part, from the Linac4 exit to the LT.BHZ20, the layout has been drawn ex-novo and the line will be housed in a newly excavated tunnel that branches out of the Linac4 –SPL tunnel towards Linac2.

The angle between the Linac4-SPL line and the point of injection in the PSB is approximately 40 degrees; however, in the impossibility of simply drawing a straight line between the two (because of the obstacle of existing structures), a more complicated and winding layout has had to be adopted.

An initial bend is needed to deflect the beam at the exit of Linac4 towards the LT-LTB line (see Fig.2 for a sketch). This is achieved by means of two consecutive identical dipoles, 1.7m in length and forming an angle of 35 degrees each, with a 0.687T applied magnetic field. They are separated by a distance of 12m and a triplet of quadrupole magnets for beam focusing.

The beam is then transported along a straight line to the LTB, over approximately 50m. Transverse focusing up to the LT.BHZ20 dipole magnet is provided by five doublets, for a total of 10, 250mm long quadrupoles having a 50mm radial aperture, peak gradient of 8T/m and integrated gradient of 2T. The quadrupoles of the three central doublets are coupled in pairs on the same power supply, whereas the two outermost ones are fed by individual power supplies in order to retain some freedom for matching the beam at the entrance and exit of this section. A debuncher cavity has been positioned after the second doublet (approximately 34m downstream Linac4) to reduce the energy spread of the beam coming out of the linac. A 1.1m long, 352MHz 5-cell cavity, with an applied voltage of 0.7MV is sufficient to match the longitudinal phase space requirements on the beam at injection in the PSB with no strong sensitivity on beam current variations.

The Linac4 transfer line joins the LT-LTB line at the position of the LT.BHZ20 magnet. In order to continue along the existing LTB path towards the PSB, the Linac4 beam is deflected at this point by an

angle of -24 degrees, and studies are under way to assess whether the present magnet could be recuperated and re-employed. After this bend and up to the injection point in the PS Booster, the line follows the path of the existing LTB-BI line: it is planned to keep all existing magnets in place, with a readjustment of their

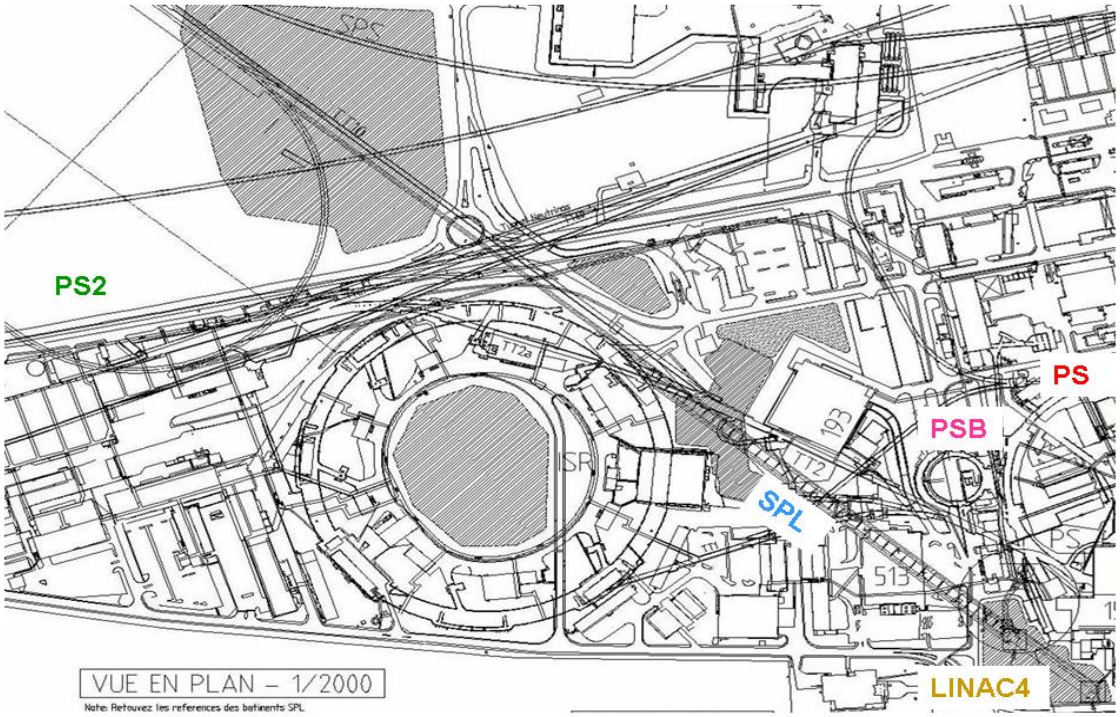

Figure 1 Green field site layout, with Linac4 and transfer line to PSB in the bottom right corner.

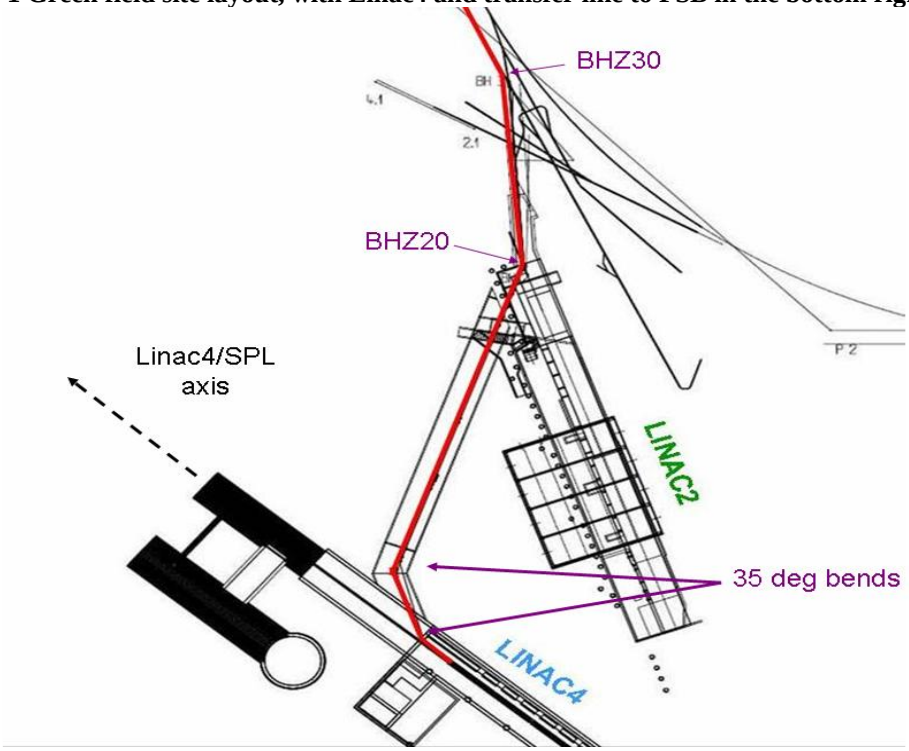

Figure 2 Transfer line layout (beam line shown in red).

transverse focusing strength to the different beam energy (therefore new power supplies will probably be required).
This final scheme has been the result of several iterations, mainly aimed at simplifying the layout, while keeping beam dynamics under control. The number and characteristics of the magnets chosen represent a minimal setup to ensure transport without losses of the nominal linac beam to the Booster, emittance and dispersion control along the transfer line and beam envelopes and dispersion matching at injection in the four PSB rings.
A Trace3D sketch of the transfer line (Fig.16) and a list of all equipment, with relative positions and specifications (Table 3), are provided in Appendix A.

Beam dynamics

a. Input beam

The initial design of the transfer line has been carried out with the program Trace3D, and was followed by more accurate multi-particle simulations with the code PATH that use for input beam either an end-to-end distribution of 45k particles obtained from tracking from the RFQ input to the end of the linac or an internally generated distribution of 50k particles with the same emittances and Twiss parameters. Figure 3 shows phase space plots for the end-to-end case, whereas Table 1 summarises the main specifications for the nominal beam at the exit of Linac4 at 160 MeV.
This has an approximately spherical shape, with widths of typically 15mm, 7mm and 9mm in the horizontal, vertical and longitudinal planes respectively (for ~90% emittance). The main purpose of beam transport in a transfer line connecting a high intensity linac to a circular machine is to provide a controlled transition from a fast phase advance regime in the linac (with frequencies in the hundreds of MHz) to a slower phase advance in the ring (1MHz for the CERN Booster), or equivalently a transition from a bunched to a more continuous type of beam. Because of the absence of longitudinal focusing, the beam in the transfer line is subject to a longitudinal debunching process and an increase in energy spread under the effect of the uncompensated space charge forces. This will eventually reach saturation after a certain distance is traveled. In presence of bending elements that introduce a non-zero dispersion to the line (and hence a coupling between the horizontal and longitudinal planes), however, the non-constant energy spread can result in an irreversible transverse emittance growth. This is particularly true in the first few metres of the Linac4 transfer line (initial bend) where a very rapid energy spread blowup and debunching take place.
Linac4 statistical error studies have been carried out to evaluate the impact on the final beam distribution of the propagation through tracking of machine errors [5]. Tolerances taken into account are on the quadrupole positions (translation and rotation, with respective RMS errors of 0.1mm and 0.5deg) and gradients (1%), on the klystron and gap fields (1%) and on the klystron phases (1deg). Results of the error simulations show an expected increase of approximately 15% in the beam transverse emittance and 20% in the longitudinal emittance due to these uncertainties. RF errors also cause a phase and energy jitter of roughly 1.8deg and 270keV (RMS values) in the final beam distribution, which need taking into account in the evaluation of the energy acceptance of the transfer line and in the setting of a sufficiently large beampipe and magnets aperture to avoid excessive beam losses.

b. Output beam

Injection into the Booster is via a multi-turn charge-exchange scheme with transverse and possibly longitudinal painting, as described in [6]. The beam delivered by the transfer line at the stripper foil position needs to be matched to the PSB closed orbit solution. In the transverse plane the baseline requirements are for $\alpha_x=\alpha_y=0$, $\beta_x=5.5$m, $\beta_y=3.8$m and minimal emittance growth. Fig.4 shows the horizontal and vertical phase space beam distributions at the end of the transfer line at the point of injection into the PSB.

Dispersion matching

Different approaches exist to dispersion matching at injection from a high-intensity linac to a circular accelerator in presence of space charge. First of all, there are two possible definitions of dispersion

function, for a full current or zero current case (with and without space charge respectively), having different time-evolutions along the transfer line. Zero current dispersion is the one which determines the beam position displacement due to some beam momentum centroid jitter.

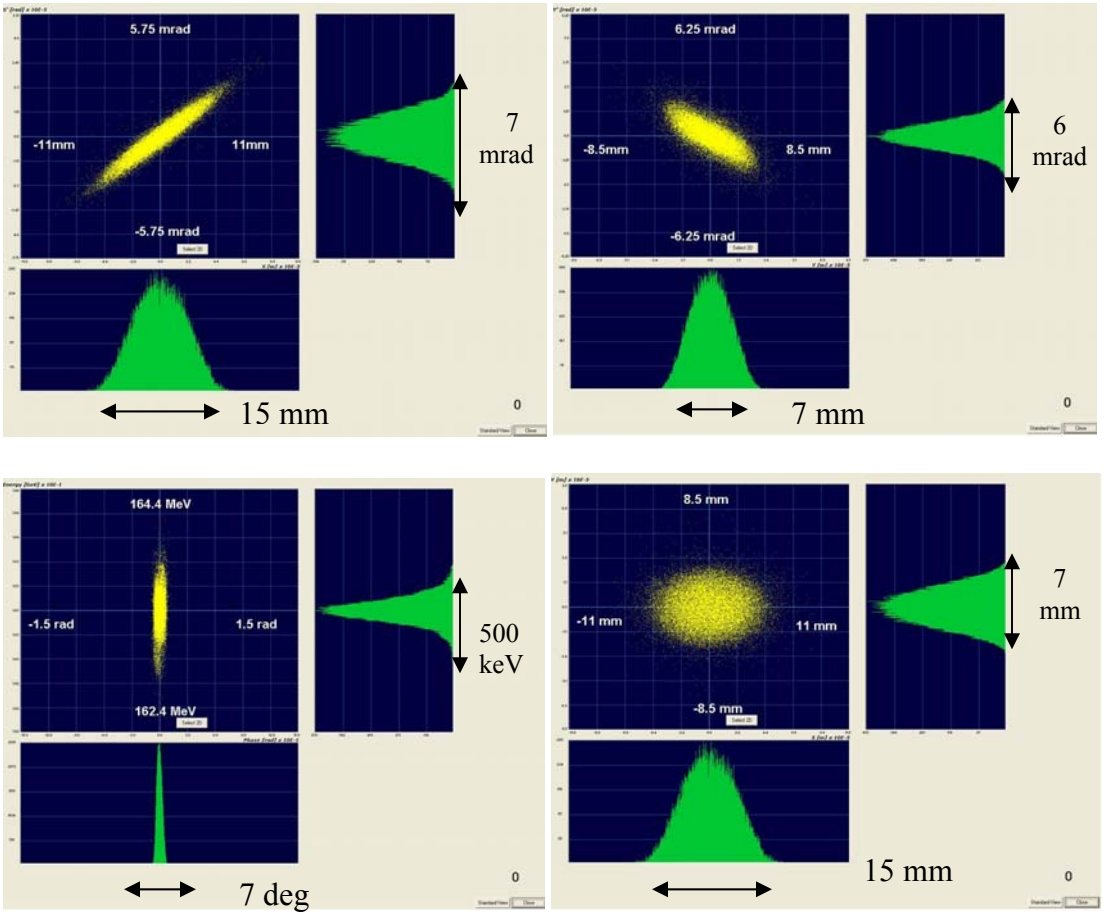

Figure 3 Phase space plots of the end-to-end input beam distribution at the beginning of the transfer line (respectively the x-x'. y-y', x-y and ΔE-Δϕ planes from the top left picture in clockwise order).

	α	β	ε RMS
x	-3.23	7.50 m/rad	0.344 mm mrad
y	1.13	2.62 m/rad	0.344 mm mrad
z	-0.12	14.29 deg/MeV	0.189 deg MeV

Energy	163.05 MeV
Current	65 mA
Frequency	352.2 MHz
Energy spread	116 keV (RMS)

Table 1 Twiss parameters and RMS normalized emittance values for the input beam distribution.

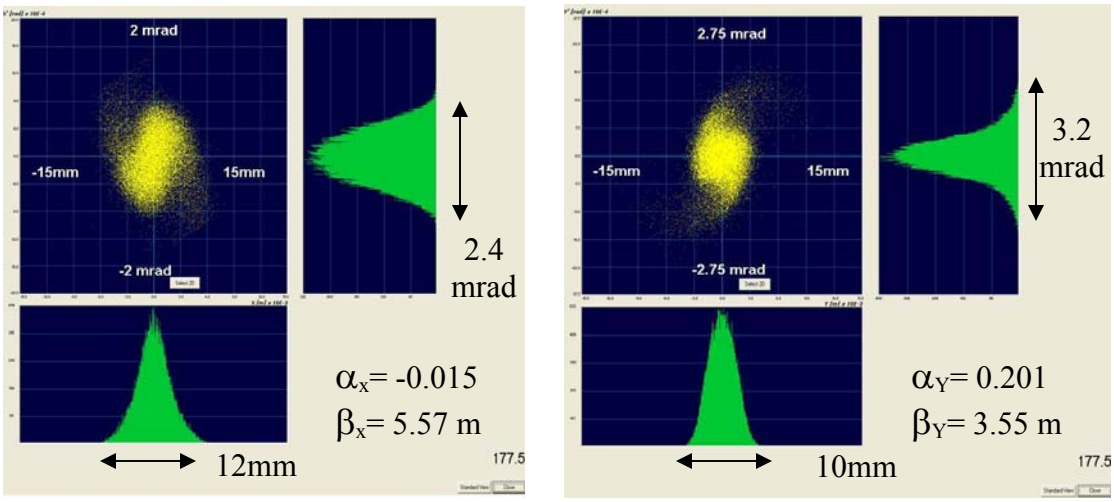

Figure 4 Horizontal (left) and vertical (right) phase space plots for the end-to-end beam distribution at the exit of the transfer line (injection foil position).

The position jitter accounts for an increase in the effective horizontal beam size at injection that can hinder complicated transverse painting schemes. However, at injection from a linac into a ring, when hundreds of linac bunches are typically packed into a single ring bucket, a certain degree of momentum jitter from bunch to bunch is unavoidable, and hence even in presence of relatively strong space charge, minimizing the zero-current dispersion at the injection point is often adopted as a solution. On the other hand, the full current dispersion turns the beam energy spread into transverse size broadening through the coupling of horizontal and longitudinal planes. To find which matching strategy is more appropriate for a certain machine, one would therefore need to assess which one between the momentum spread and the momentum jitter contributes most to the beam emittance growth.

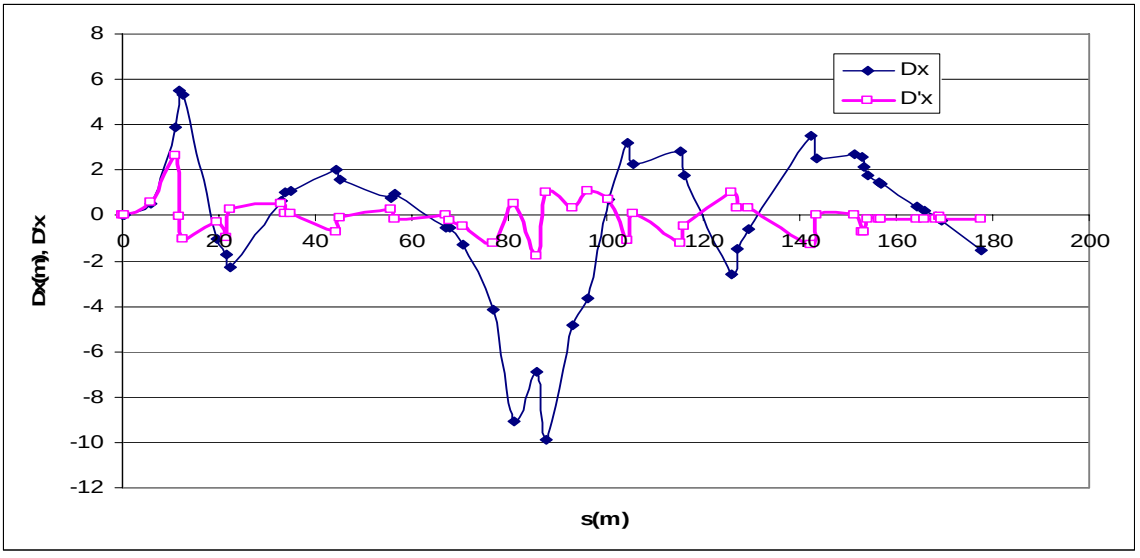

Figure 4 Evolution of the zero current dispersion function and its derivative along the Linac4 transfer line.

For the present 170mA Linac2 beam injection in the PSB (at 50 MeV and final energy spread of 200keV for a 90% emittance, equivalent to a 0.2% $\Delta p/p$), a recent campaign of studies and measurements [7] has shown that the efficiency of multi-turn injection could be considerably increased by re-matching to zero the dispersion at the end of the line and its derivative (thus reducing beam losses at injection and during the first few turns by decreasing the beam size). For the Linac4 beam (65mA at 160MeV and with a 270keV

energy spread for 90% emittance at injection, corresponding to 0.08% Δp/p) we expect the beam momentum jitter contribution to be predominant over the beam energy spread and space charge effects. Therefore in the present we have studied the evolution of the zero current dispersion along the transfer line, and considered that for the final matching requirements. The closed orbit dispersion solution in the PSB at the injection point gives D_x=-1.42m (MAD-X sign convention for protons) and D'_x=0. Two possible matching scenarios are envisaged: a fully matched case, with D_x=-1.42m at the end of the transfer line, and a mismatched case with D_x=0. In the first scheme, off-momentum bunches would impact on the injection foil at different locations: one would therefore need a foil with a larger surface, but on the other hand there would be no transverse emittance increase in the beam because of the precise matching. In the second scheme, instead, all bunches would hit the same region of the foil, but the dispersion mismatch would cause some emittance blowup, which would be correlated with the longitudinal phase space. Preliminary studies [8] have shown that the emittance growth in this second solution would fail to satisfy the requirements on beam size and emittance for an LHC-type beam, hence the first matching scenario has been here adopted. Fig. 5 shows the evolution of the zero current dispersion function and its derivative along the transfer line, up to injection in the PS Booster.

Multi-turn injection in the PSB, on ramp with $\partial B\rho/\partial t$=10Tm/s, $V_{h=1}$=8kV and $V_{h=2}$5kV, defines a bucket height of ΔE=±1.2MeV[9]. Even without any longitudinal manipulation during transfer from the linac, but just letting the beam de-bunch under the effect of the space charge forces, the final energy spread on target is around 314 keV RMS (or 540 keV for 90% emittance), much smaller than the total acceptance available.

At present a Linac2-type solution is being followed as base for the longitudinal beam dynamics, with the use of a debunching cavity that reduces the beam energy spread. Fig. 6 to the left shows the evolution of the RMS values of the energy spread and phase width for this solution, reaching approximately 150 keV and 50deg at the PSB injection point. The longitudinal phase space beam distribution at the end of the transfer line is illustrated in Fig.6 to the right.

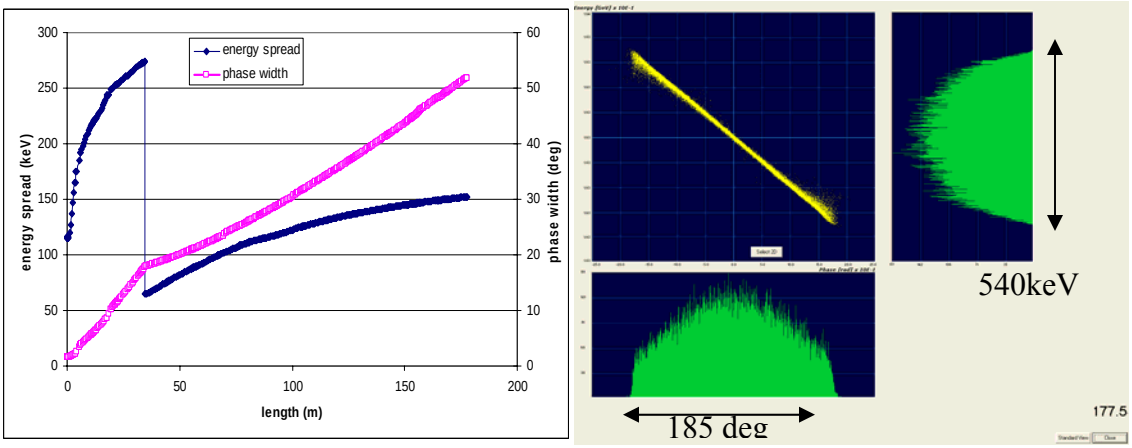

Figure 6 Evolution of the RMS energy spread and phase width along the transfer line (blue and purple curves respectively, to the left), and longitudinal phase space distribution at the injection point in the PSB (right).

Longitudinal painting

A longitudinal painting strategy during injection is under study to achieve a more homogeneous particle distribution into the PSB bucket with a consequent increase in the bunching factor and an improvement of the capture efficiency, quantitatively equivalent to the effects of an increase in the injection energy.

The implementation studied involves a slow triangular energy modulation at the end of Linac4 from -1.2 MeV to +1.2 MeV over a half-period of 10 PSB revolutions: the PSB bucket would be thus scanned ten times at different increasing energies and ten times with decreasing energies over its full acceptance (see Fig.7). After chopping, roughly 222 linac bunches with a 352MHz time structure would fill the 1MHz PSB bucket per sweep.

The energy modulation could be realized by ramping within a ±10% range the field in the last two PIMS cavities of Linac4[10]. The deviation in energy from the nominal case will produce variations in the phase

advance rate along the transfer line and consequently a relative de-phasing of the bunches with respect to the on-momentum bunch. This effect has to be accounted for in relation to the other, debunching cavity downstream, that will have to follow in time the phase shift to ensure that all bunches 'see' the same voltage upon their passage.

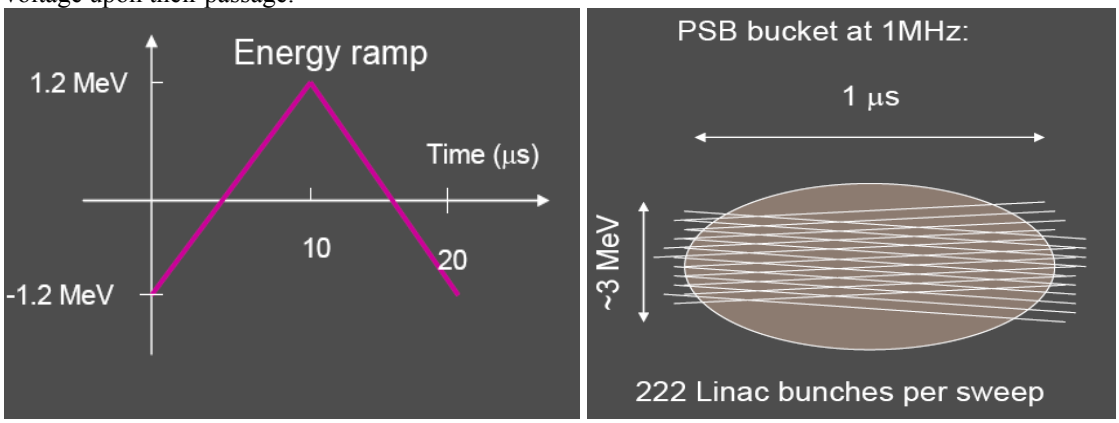

Figure 7 Scheme of triangular energy modulation for longitudinal painting at the PSB injection (left), and PSB bucket filling scheme (right).

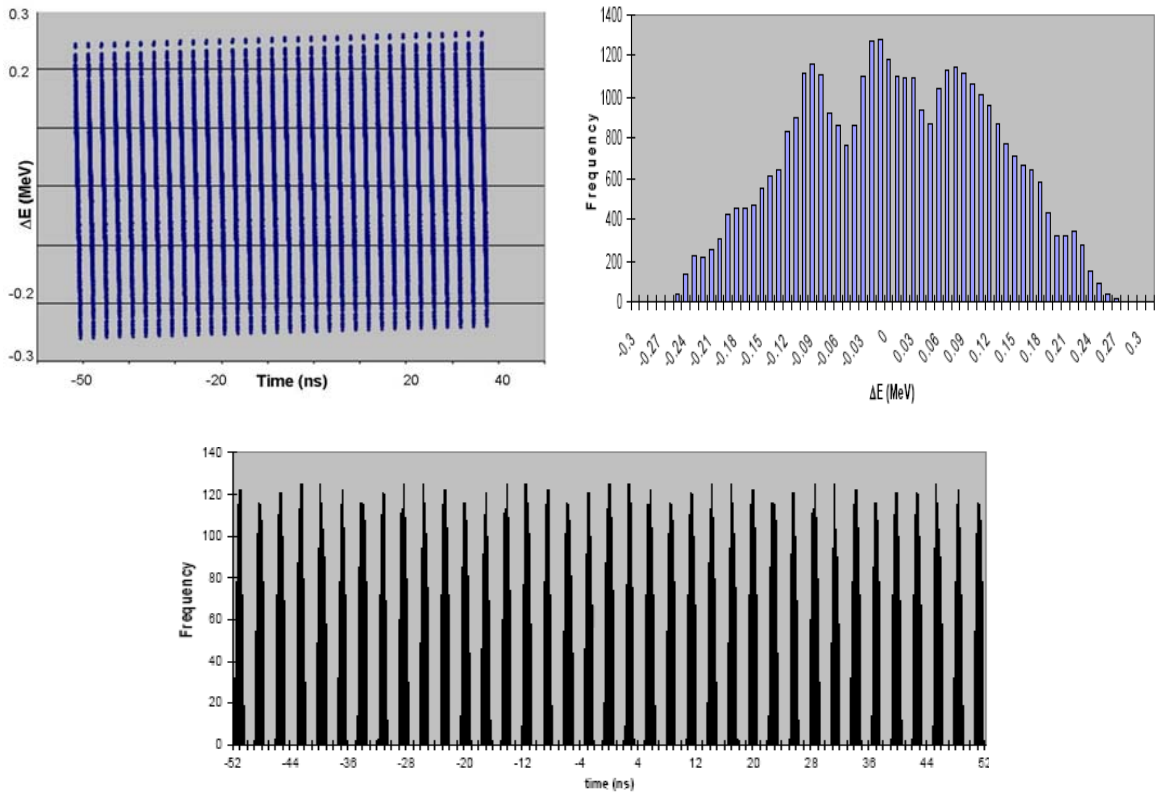

Figure 8 Longitudinal filling of a PSB bucket over a 0.1μs snapshot of the injection process (top left), and energy spread and phase projections of the final accumulated beam distribution in the PSB (top right and bottom picture respectively).

Figure 8 shows a snapshot of the injection process with energy modulation over a time window of 0.1 μs centred around the on-momentum bunch: on the top left is the longitudinal phase space as 'seen' by the PSB with a succession of linac bunches at 352MHz sweeping the bucket (here the dephasing due to the energy ramping has been omitted because it is negligible on a bunch to bunch timescale of 2.85ns). The top

right and bottom pictures show the energy and phase spectra of the particles: since the single bunch coming from the linac is not completely debunched at the end of the transfer line (see Fig.6 right) but occupies only about half the total width of the 352MHz bucket, a memory of the 352MHz bunch structure will remain in the 1MHz PSB bucket with the presence of phase gaps in the beam distribution. Further studies will need to assess whether this 352 MHz structure has any consequences on the injection efficiency and could be avoided by relaxing the constraints on the debuncher cavity to achieve a larger energy spread of the beam.
The modulation in energy of the Linac4 bunches has an immediate impact on the transverse planes at injection and on the transfer line acceptance. In the case of non perfect dispersion matching between the transfer line and the Booster, any momentum offset of the beam will be converted into a shift from the origin in the transverse horizontal phase space, which could affect the transverse painting scheme at injection.
In the transfer line on the other hand, the same effect will cause a movement off-axis of the beam centroid with a consequent effective reduction in the line acceptance, as calculated for an on-momentum beam.
Fig.9 shows the horizontal deviation of the beam center for a shift in energy of 1.2 MeV, endpoint of the energy ramping scheme studied (in yellow), together with the 5RMS beam envelopes (in blue) in comparison with the physical aperture limits of the transfer line (in purple) as previously defined (a provisional 50mm radius aperture for the part to be newly built and the values currently in place for the rest). Clearly a bottleneck is present in the tract of the line with the highest dispersion (between the

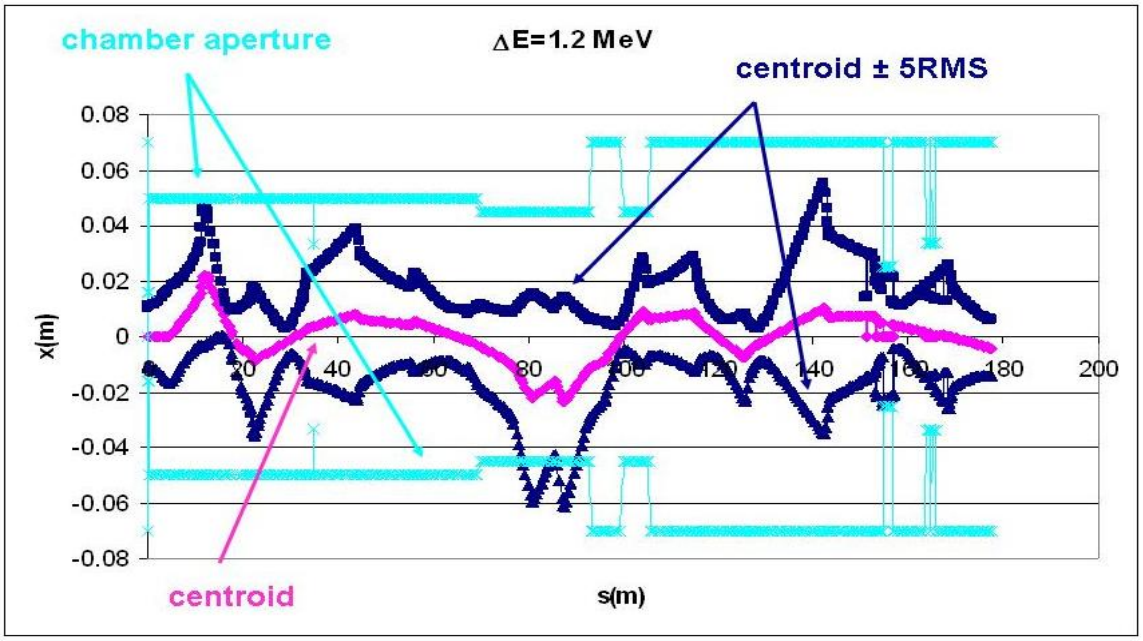

Figure 9 Line acceptance for a 1.2 MeV energy shift: horizontal deviation of the beam center (purple), with 5RMS beam envelopes (blue lines), compared with the physical aperture of the transfer line (in cyan).

LT.BHZ20 and LT.BHZ30 dipoles) with a consequent high potential for beam losses; a retuning of the line might therefore be necessary to reduce the dispersion bump or else the production of new magnets with a more generous bore radius. Adding to the energy shift introduced by the longitudinal painting, one should also consider the contribution of the energy jitter caused by the propagation through the linac of longitudinal RF errors. As mentioned before, RF machine errors with a 1%-1deg RMS distribution determine an uncertainty in the longitudinal phase space at the end of the linac of 271keV and 1.8deg (RMS values). Even though there are indications that this could be a conservative estimate and that we could possibly relax the error amplitudes to 0.5%-0.5 deg, the Low-Level RF system for Linac4 has not been studied in sufficient detail yet to justify a less pessimistic approach for the time being. The energy

acceptance of the line has been evaluated by studying how transmission drops as a function of an energy shift applied to the input beam distribution (see Fig.10).
The maximum tolerance of the line is for just over a 1% variation in the nominal beam energy: the beam would be completely lost for an energy shift of 2MeV, corresponding to the sum of the largest longitudinal painting amplitude and three times the RMS size of the jitter due to RF errors.
Apart from lowering the transfer line acceptance limits, the energy jitter effect could also be a potential showstopper for the longitudinal painting solution itself, if the dependency of the energy offset as a function of time cannot be controlled. It's consequently not just important to better understand and quantify the effect of RF errors, but also to establish whether they occur on a pulse-to-pulse or rather bunch-to-

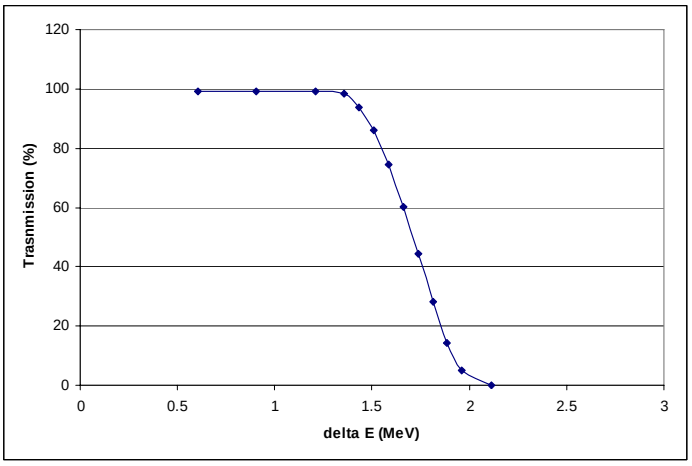

Figure 10 Energy acceptance of the transfer line, given in terms of transmission values as a function of the beam centroid momentum shift.

bunch scale and whether they are of a reproducible nature (and therefore possible to compensate via some feedback system) or rather random and uncorrectable.

c. Beam transport

The first part of the transfer line, with the bend towards the LTB line, has proved to be very critical from a beam dynamics point of view. A locally achromatic solution was initially attempted by using the quadrupoles of the triplet nested between the two dipoles to match the zero current dispersion and its derivative to zero at the exit of the bend. This however could not prevent some transverse emittance blowup due to the very rapid increase in the beam energy spread all along this part in presence of dispersive elements. Since space charge effects are predominant at this point, controlling the emittance growth (or rather the full current dispersion, inclusive of space charge), as an intrinsically irreversible process, is more crucial than minimizing the zero current dispersion and its derivative (which can be later achieved with some matching downstream). For this reason an empirical tuning of the triplet gradients was carried out to find the settings that minimize the transverse emittance growth along this tract of the line, and these values were then assumed regardless of the residual dispersion at the end.
A straight transport section follows the initial bend up to the point of intersection with the LTB line. A doublets structure has been chosen for this part, in order to keep to a minimum the number of magnets used (with 10m long drifts between adjacent cells), while at the same time providing a very regular focusing scheme for the beam dynamics. The first and last doublet are used to match the beam at the entrance and exit of this section. A debuncher cavity has also been introduced at this point to reduce the energy spread of the beam coming out of the linac. Its position (at about 35m from the linac exit) has been chosen as a balance between letting the growth in energy spread under space charge effects reach saturation, and avoiding the introduction of RF non-linearities that occur when the beam phase width is larger than the linear region of the RF slope.
After coming up to the LT.BHZ20 dipole, the beam follows the path of the Linac2 transfer line, and all existing magnets have been kept in place with a readjustment of their gradients.

The six quadrupoles between the LT.BHZ20 and LT.BHZ30 dipoles are the most efficient knobs for tuning the dispersion at the point of injection in the PSB.
Fig.11 shows the relative shift from the nominal case in the final zero-current dispersion values due to a ±5% and ±10% change in each one of the quadrupoles' gradients (varied one by one). LT.QDN55, LT.QFN60 and LT.QDN65 are the magnets giving larger excursions, and therefore the most effective for tuning.

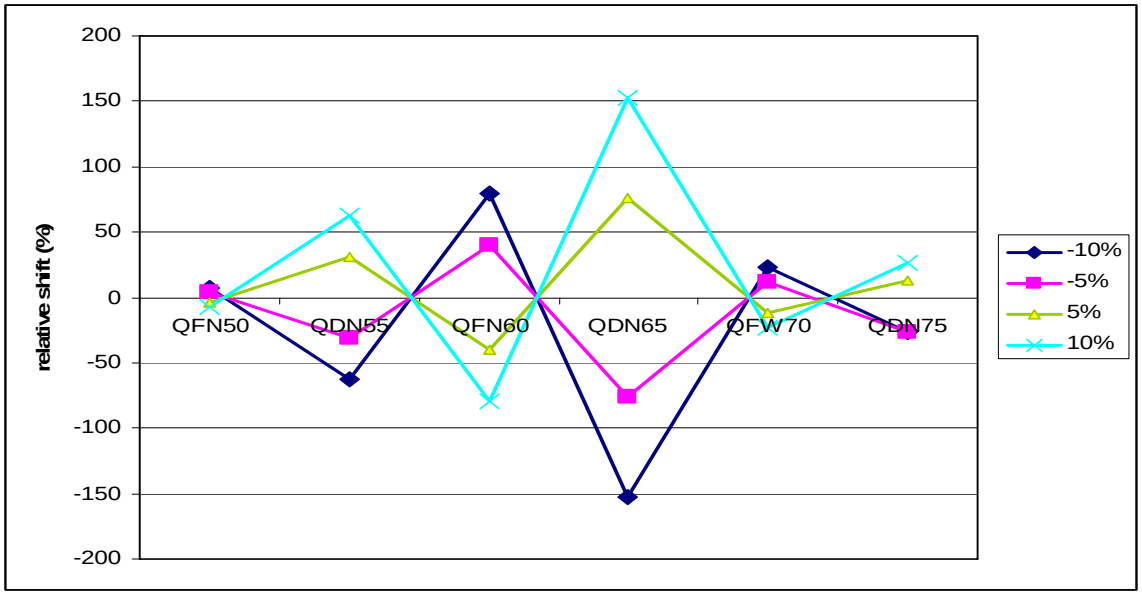

Figure 11 Relative excursion from the nominal case of the dispersion values at PSB injection when changing each one of the quadrupoles'gradients (between the LT.BHZ20 and LT.BHZ30 dipoles) by ±5% and ±10%.

In the BI line the beam is distributed to the four Booster rings by a vertical bending magnet (DVT30), a system of five kicker magnets (DIS), another vertical bend (DVT40) and 3 septum magnets (SMV). The beam enters the distributor with a vertical beam offset of 5.2mm (created by DVT30 and an extra vertical dipole placed on the other side of the BI.QN030 quadrupole) and is then sequentially deflected by the combined action of the DIS, DVT40 and SMV into the four separate apertures of the BVT dipole magnet, to achieve the required PSB beam level separation of 360mm between each ring (see the sketch in Fig.12).
The injection equipment and the beam deflection mechanics have been included and modeled in the PATH simulations for the four different ring cases.

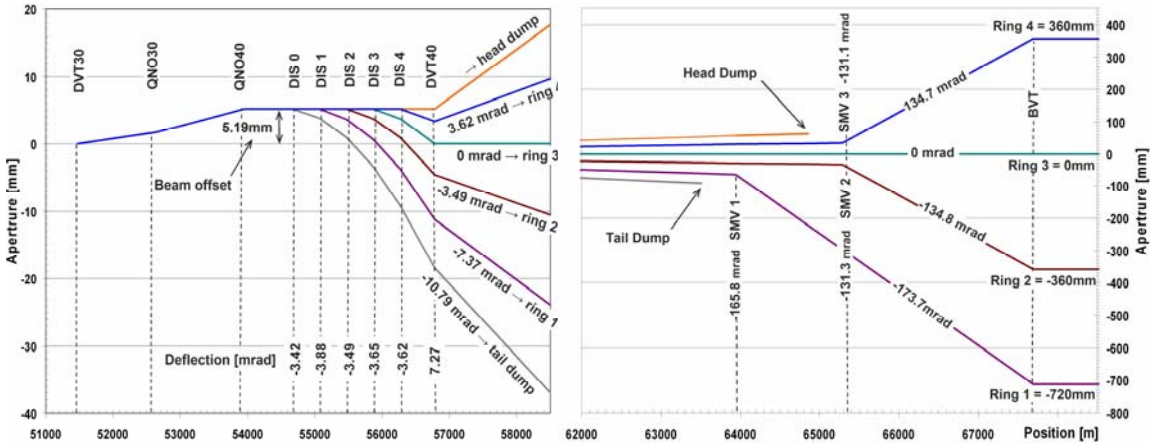

Figure 12 Sketch of the beam distribution system into the four PSB rings [11].

The six quadrupole doublets in the LTB-BI part of the line following the LT.BHZ30 dipole have been used for modulating the beam envelopes to match the arrival conditions at the Booster, as previously specified. Fine tuning studies have been aimed at finding the closest possible injection match for the case of the beam in Ring3 (which suffers the least deflection), by means of iteratively matching the zero-current dispersion values and the full-current transverse Twiss parameters until satisfactory convergence.

	Ring1	***Ring2***	***Ring3***	***Ring4***
α_x	0.101	0.067	-0.015	0.068
α_y	-0.929	-0.658	-0.201	-0.657
β_x (m)	7.35	6.66	5.57	6.66
β_y (m)	5.45	4.22	3.55	4.21
D_x(m)	-1.49	-1.50	-1.50	-1.50
D'_x	-0.16	-0.16	-0.16	-0.16
D_y(m)	0.10	0.014	0	-0.015
D'_y	0.13	0.06	0	-0.06

Table 2 Final beam parameters at injection point in the PS Booster: dispersion values are calculated for a zero-current case, wehereas the Twiss parameters have been obtained for a 65mA current case. The results are from simulations using an end-to-end beam distribution.

The quadrupole settings found for this case have been then extended to all the other rings, obtaining only slight variations in the final matching values (see Table 2).

PATH simulation results for a through tracking in the transfer line with an end-to-end initial beam distribution and 2D space charge approximation are shown in Figs.13-14. Transverse RMS beam sizes are mostly contained within 6mm (Fig.13 left); the emittances shown in Fig.13 to the right are inclusive of the combined contribution of energy spread and dispersive effects (as can be seen in the 'steps' occurring at the dipole positions for the horizontal plane).

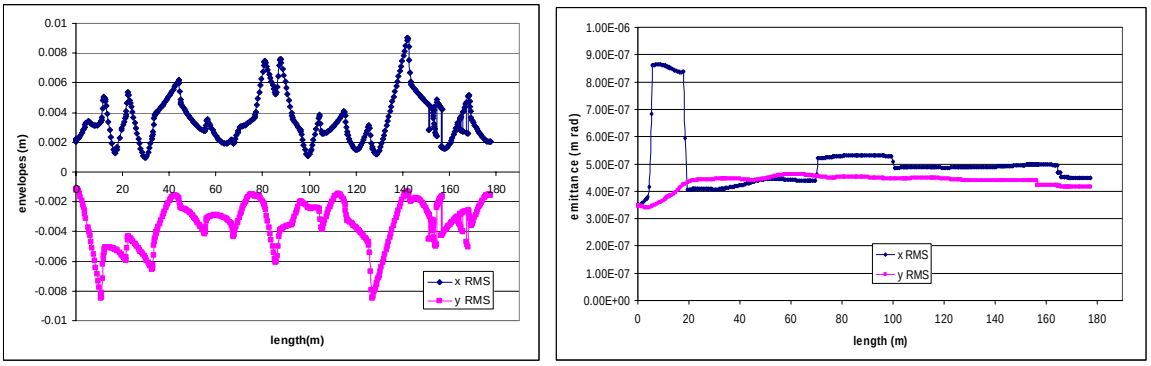

Figure 13 Transverse RMS beam envelopes (left) and emittances (right).

The overall growth along the whole 180m length of the transfer line can be contained within 28% and 20% respectively for the horizontal and vertical planes, with final normalized RMS values of 0.45 and 0.42 π mm mrad. It's been observed however that most of this growth is in fact due to halo propagation: by applying some collimation on the initial beam distribution coming out of the linac (see Fig.15), one can already reduce the emittance increase to 22% horizontally and 8% vertically (for 96.5% of the particles).

There are no large asymmetries in the two transverse beam sizes (Fig.14 left) along most of the transfer line and the aperture radius to RMS beam size ratio (Fig.14 right) has been almost always kept above a lower limit of 5 for an on-momentum beam (assuming an aperture of 50mm radius in the part of the transfer line to be newly built, and the current aperture values for the rest, i.e. approximately 45mm radius up to the LT.BHZ30 and 70mm downstream).

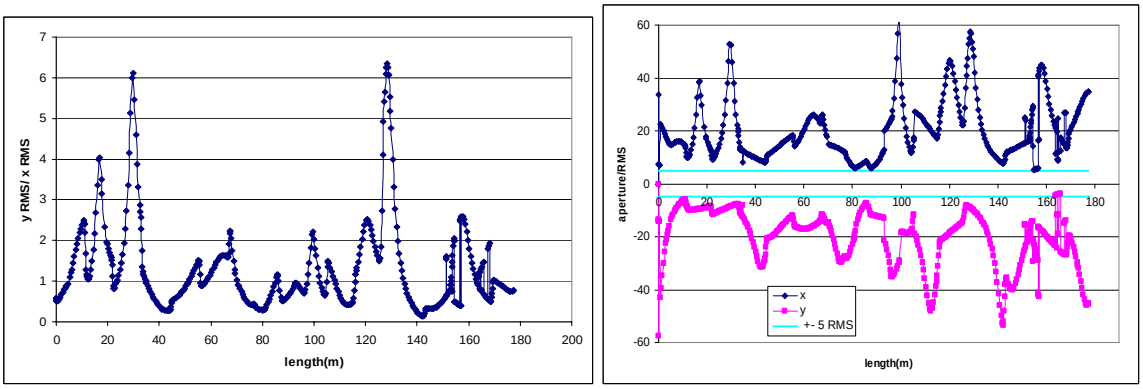

Figure 14 Beam aspect ratio (left) and aperture radius to RMS beam size ratio (right) .

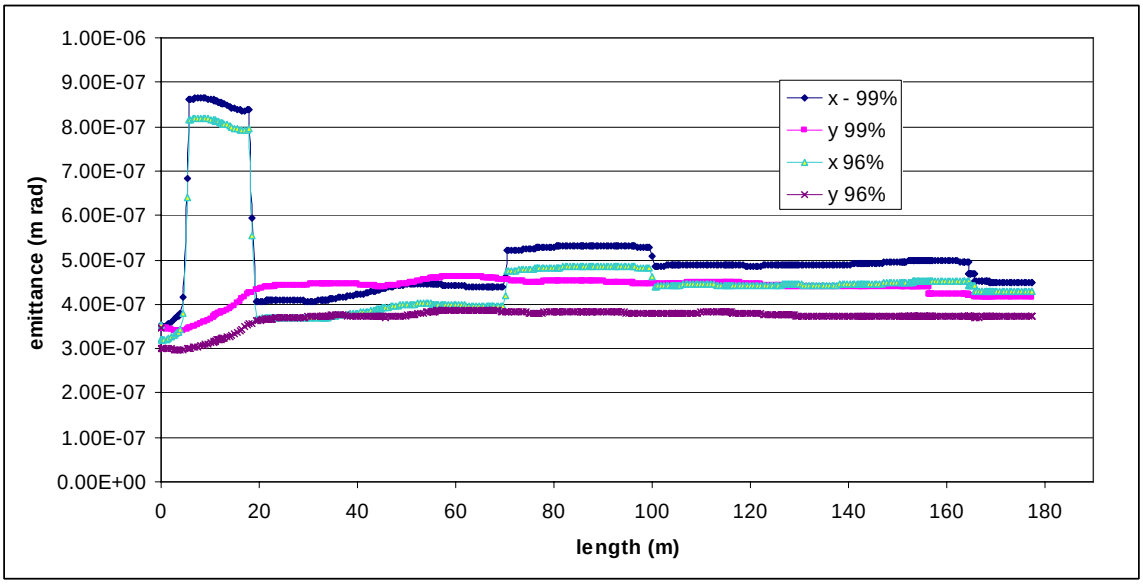

Figure 15 Comparison of RMS transverse emittances growth for 96% and 99% of the beam (with and without some initial collimation on the beam distribution coming out of the linac), showing the effects of beam halo during transport through the transfer line.

Conclusions

In conclusion, a solution has been here presented for the design of a transfer line to transport the beam at the exit of Linac4 to the PS Booster in a newly selected site in proximity of the Mont Citron. Beam transport along the nearly 200m of line has been achieved with no losses and controlled transverse emittance growth. Matching conditions at the PSB have been satisfied, and where these have not been precisely specified yet (as in the case of the dispersion matching) enough flexibility has been built in the line to allow tunability for different values of the parameters.

The energy acceptance of the line is being evaluated in relation to the latest estimates on beam jitter caused by RF errors in the linac, and also in relation to longitudinal painting schemes currently under study for beam injection into the PSB. If the range in energy shift assumed for the results here presented is in fact confirmed, further tuning will be needed to reduce the peaks in the dispersion function along the line causing acceptance bottlenecks.

Finally a whole collimation strategy has still to be devised to both achieve a better beam quality by eliminating the halo propagated down from the linac (and the transverse emittance growth associated) and also to reduce beam losses and activation levels along the line.

References

[1] G.Bellodi, A.Lombardi, "Transfer Line Studies from LINAC4 to the PS Booster : "South Hall" Option", CERN-AB-Note-2007-004 (2007).
[2] "Linac4 Technical Design Report", CERN-AB-2006-084 (2006).
[3] "Conceptual design of the SPL II", CERN-2006-006 (2006).
[4] M.Benedikt, "General design aspects for PS2", CERN 2007-002 (2007).
[5]M.Baylac,"Error studies of Linac4", presentation at ICFA-HB2006 workshop.
[6] M.Martini, C.R.Prior, "High-intensity and high-density charge-exchange injection studies into the CERN PS Booster at intermediate energies", EPAC 2004 Proceedings, (2004).
[7] K.Hanke *et al*, "Dispersion matching of a space-charge dominated beam at injection into the PS Booster", PAC 2005 proceedings (2005).
[8] B.Goddard, private communication.
[9] C.Carli, private communication.
[10] E. Sargsyan, private communication.
[11] W.Weterings et al.,"160 MeV H- injection into the CERN PSB", PAC2007 Proceedings (2007).

Appendix A

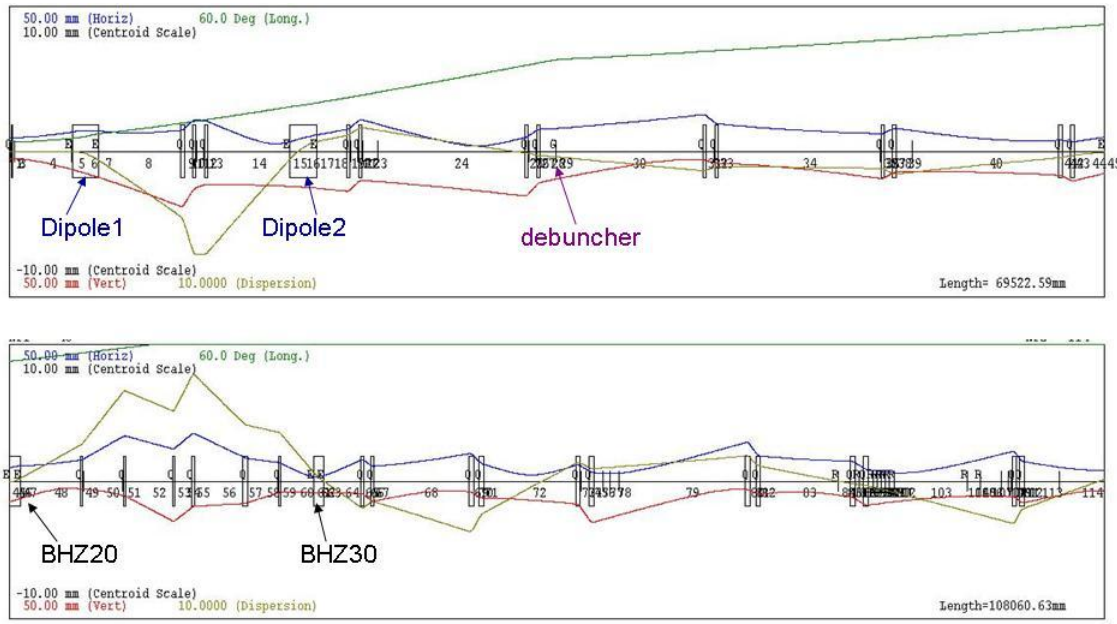

Figure 16 Sketch of the transfer line showing magnet positions, beam envelopes (blue and red lines), longitudinal phase spread (in green) and dispersion (in ochre). The top plot shows the 'new' part of the transfer line, the bottom one shows the part along the Linac2 transfer line up to the PSB.

Element	s (m)	Magnetic length (mm)	Gradient (T/m)	Angle (deg)	Voltage (MV)
Dipole1	4.8	1710		35	
Quad1	11	250	4.32		
Quad2	11.75	250	-3.82		
Quad3	12.5	250	-1.34		
Dipole2	18.67	1710		35	
Quad4	21.55	250	3.26		
Quad5	22.3	250	-4.21		
Quad6	32.85	250	3.45		
Quad7	33.6	250	-3.45		
Debuncher1	34.7	1150			0.7
Quad8	44.15	250	-3		
Quad9	44.9	250	3		
Quad10	55.45	250	3.2		
Quad11	56.2	250	-3.2		
Quad12	66.75	250	-2.23		
Quad13	67.5	250	3.10		
LT.BHZ20	70.1	1094		-24.1	
LT.QFN50	76.7	255	1.42		
LT.QDN55	80.9	255	-1.43		
LT.QFN60	85.8	255	2.52		
LT.QDN65	87.7	255	-2.09		
LT.QFW70	92.8	467	0.5		
LT.QDN75	96.2	255	-1.50		
LT.BHZ30	100.1	1006		-22	
LTB.QFN10	104.4	255	-4.12		
LTB.QDN20	105.4	255	3.83		
LTB.QFW30	115.1	461	-1.81		
LTB.QDW40	116.1	461	1.54		
LTB.QFW50	125.7	461	-2.33		
LTB.QDW60	127	461	1.80		
BI.Q10	142.42	462	-1.84		
BI.Q20	143.42	462	2.07		
BI.Q30	152.7	462	-1.26		
BI.Q40	154	462	1.39		
BI.Q50	168.8	466	-2.25		
BI.Q60	169.55	466	2.24		
end	177.7				

Table 3 Specifications of the transfer line elements. From left to right: the longitudinal coordinate of the center (m), the magnetic length (mm), quadrupole gradients (T/m), dipole bending angles (deg) and debuncher voltages (MV).